Exact Similariton solution families and Diverse Composite Waves in Coherently Coupled Inhomogeneous Systems

Kui Huo[1], Rongcao Yang[1,2,], Heping Jia[1], Yingji He[3], J.M. Christian[4]*

[1] School of Physics & Electronic Engineering, Shanxi University, Taiyuan, 030006, China

[2] Collaborative Innovation Center of Extreme Optics, Shanxi University, Taiyuan, 03006, China

[3] School of Photoelectric Engineering, Guangdong Polytechnic Normal University, Guangzhou, 510665, China

[4]Joule Physics Laboratory, School of Science, Engineering and Environment, University of Salford, Greater Manchester, M5 4WT, UK

**Email:sxdxyrc@sxu.edu.cn*

Abstract Seeking analytical solutions of nonlinear Schrödinger (NLS)-like equations remains an open topic. In this paper, we revisit the general inhomogeneous nonautonomous NLS (inNLS) equation and report on exact similaritons under *generic* constraint relationships by proposing a novel *generic* self-similar transformation, which implies that there exist a rich variety of highly-controllable solution families for inhomogeneous systems. As typical examples, richly controllable behaviors of the self-similar soliton (SS), self-similar Akhmediev breather (SAB), self-similar Ma breather (SMB), and self-similar rogue wave (SRW) are presented in a periodic distribution nonlinear system. With the aid of a linear transformation, these novel similariton solutions are deployed as a basis for constructing two-component composite solutions to a pair of coherently coupled inNLS equations including four-wave mixing. The diverse composite waves that emerge, including SS–SS, SAB–SMB, and SRW–SRW families, are investigated in some detail. The family of similariton solutions presented here may prove significance for designing the control and transmission of nonlinear waves.

Key words: generic self-similar transformation; exact similaritons family; diverse composite waves; control and transmission

1. Introduction

Similaritons in amplifying nonlinear graded-index waveguides can be realized under much less compatibility condition by controlling the power of Raman gain to match the parameters of the waveguides [1]. This line of work has been extended in various ways to nonautonomous systems [2, 3]. Similar results have also been obtained for matter waves in trapped or anti-trapped Bose-Einstein condensates (BECs) with time-modulated atomic interactions [4]. The transmission of nonlinear waves in inhomogeneous waveguide systems are well described by an inhomogeneous

nonautonomous nonlinear Schrödinger (inNLS) equation [5, 6]. Many works have been devoted to finding solution constructions of inNLS-like equations with recourse to methods such as Darboux transformations and Lax pairs [7-9], Hirota bilinearizations [10], and self-similar transformations [10-14]. To date, some important self-similar soliton solutions have been obtained under special balance conditions between gain/loss, dispersion and nonlinearity [5-20]. Motivated by these works, it is natural to pose two key questions: (i) *Are there other self-similar solutions of inNLS-like equations that have not yet been found?* (ii) *Do there exist families of solutions that can describe the dynamics of solitons and/or similaritons for various inhomogeneous systems?* In this paper, a series of exact similariton solutions of an inNLS equation with external potentials will be sought by introducing a *generic* self-similar transformation and a *generic* constraint relationship between gain/loss, dispersion and nonlinearity. The arbitrary nature of the parameters and the introduction of a matching function representing residual gain/loss can be expected to give rise to similariton solutions with a diverse range of forms.

In more sophisticated geometries, coupled NLS/inNLS equations can model physical processes that support multiple or multi-component nonlinear waves [16-21]. For instance, Manikandan *et al.* [16] investigated the manipulation of vector localized matter waves in multi-component Bose-Einstein condensates by transforming coupled inNLS equations into constant-coefficient NLS equations. Babu Mareeswaran *et al.* [17] analyzed superposed nonlinear waves of coherently coupled inNLS equations in systems with periodic and kink-like nonlinearity distributions. More recently, Jia *et al.* [18] have investigated coherently coupled inNLS equations through three kinds of similarity transformations, demonstrating energy exchange and the existence of a wide selection of composite waves in homogeneous/inhomogeneous optical fiber systems. Also of particular note is the work of Ding *et al.* [7], who presented breathers and rogue waves for coupled inNLS equations with the aid of Darboux transformations in the context of inhomogeneous plasmas.

Here, we will use a linear transformation of envelopes to help identify families of similaritons that satisfy the inNLS equation. Those single-component solutions can then be mapped onto two-component solutions for a pair of coherently coupled inNLS equations. Subsequent analysis will focus on the propagation and control of various composite waves in inhomogeneous coupled systems.

The significance of the results presented in this work is threefold:

i) A family of exact similariton solutions for an inNLS equation involving external potentials is

presented by proposing introducing a *generic* self-similar transformation with a *generic* constraint relationship among gain/loss, dispersion and nonlinearity.

ii) The *generic* constraints imply that there always exist exact similaritons with quite different forms in inhomogeneous fibers even if gain/loss, dispersion and nonlinearity are not precisely balanced. As illustrative examples, the control of typical similaritons in inhomogeneous systems will be demonstrated.

iii) The family of similaritons can also be applied, via a linear transformation, to coherently coupled inNLS equations. The implication is that there must also exist corresponding series of *composite self-similar waves* in inhomogeneous coupled systems.

The analysis presented in this paper is organized as follows. In Section II, we derive a family of exact similariton solutions of an inNLS equation with external potentials by proposing a novel *generic* self-similar transformation. The dynamics of those new solutions is demonstrated in Section III, where we consider the propagation in a range of inhomogeneous nonlinear fibers. In Section IV, we use a linear transformation to decouple a pair of inNLS equations including four-wave mixing terms into two identical inNLS equations. Utilizing the family of similaritons solutions (obtained in Section II), we study a broad range of composite self-similar waves in a coherently coupled inNLS model with periodic nonlinearity and different residual gain/loss. We conclude, in Section V, with some discussions of our results.

2. A family of similariton solutions of inNLS equation

Nonlinear waves such as optical solitons, rogue waves, and matter wave solitons in homogeneous systems can be well described by the NLS equation [22-26]. In realistic applications, systems are rarely homogeneous due to long-distance transmission, manufacturing imperfections, and the inclusion of other technological elements (e.g., connected to soliton management and control). It is necessary, then, to investigate how these types of nonlinear waves arise in non-autonomous inhomogeneous systems, and how they evolve during interactions in the presence of external potentials. The transmission of nonlinear waves in inhomogeneous systems can be modelled by the following inNLS equation [5, 6, 27, 28]:

$$i\frac{\partial u}{\partial z}+d(z)\frac{\partial^2 u}{\partial t^2}+2r(z)|u|^2u+[\Omega_0(z)+\Omega_1(z)t+\Omega_2(z)t^2]u+i\Gamma(z)u=0. \quad (1)$$

Here, $u \equiv u(z, t)$ is the envelope of the electric field while z and t represent the longitudinal (spatial) and time coordinates, respectively. The real functions $d(z)$, $r(z)$ and $\Gamma(z)$ describe the group-velocity dispersion, nonlinearity, and gain ($\Gamma(z) < 0$) or loss ($\Gamma(z) > 0$) in the system, respectively. The real function $\Omega_0(z)$, $\Omega_1(z)$ and $\Omega_2(z)$ parametrize the constant, linear and parabolic contributions, respectively. Equation (1) is of technical interest because of its wide range of potential applications [3-6, 13, 29, 30]. It can be used to investigate not only the stable transmission of optical pulses in inhomogeneous fiber or waveguide systems, but also the amplification and management of solitons and combined waves [10, 20, 21]. Over recent years, some particular similariton solutions of Eq. (1) have been found for special constraints [12, 18, 31-36]. Here, we are interested in more general analytical solutions of Eq. (1) under somewhat relaxed conditions. To proceed, we propose a generic self-similar transformation

$$u(z,t) = A(z)q(Z(z),T(z,t))e^{i\varphi(z,t)}, \tag{2}$$

with

$$A(z) = k_1 \frac{r(z)^{\lambda_r}}{d(z)^{\lambda_d}} e^{-g(z)}. \tag{3}$$

The real functions $Z(z)$, $T(z,t)$, $A(z)$ and $\varphi(z,t)$ represent the effective propagation distance, self-similar time, self-similar amplitude and self-similar phase variables of the similariton, respectively. Parameters k_1, λ_d and λ_r are arbitrary real constants, and $g(z)$ quantifies the gain/loss. Equation (3) implies that $A(z)$ is proportional to either $[r(z)/d(z)]^{1/2}$ or $[r(z)d(z)]^{1/2}$, which embodies the expectation that growth or decay of the amplitude due to gain/loss should be exponential along the transmission direction z [12, 18, 32]. Inserting Eqs. (2) and (3) into Eq. (1) and imposing the following conditions

$$Z_z = k_1^2 \frac{r(z)^{2\lambda_r+1}}{d(z)^{2\lambda_d}} e^{-2g(z)}, \quad T_t = k_1 r(z)^{\lambda_r+\frac{1}{2}} d(z)^{-\lambda_d-\frac{1}{2}} e^{-g(z)}, \tag{4}$$

$$d^2(z)\varphi_{tt} r(z) - \lambda_d r(z) d_z(z) + d(z)[\Gamma(z) r(z) - r(z) g_z(z) + \lambda_r r_z(z)] = 0, \tag{5}$$

$$T_z + 2d(z) T_t \varphi_t = 0, \tag{6}$$

$$-\varphi_z - d(z)\varphi_t^2 + V(z,t) = 0, \tag{7}$$

where the subscripts z and t denote derivatives with respect to those variables and $V(z, t) = \Omega_0(z)+\Omega_1(z)t+\Omega_2(z)t^2$, one can obtain the standard NLS equation,

$$i\frac{\partial q}{\partial Z}+\frac{\partial^2 q}{\partial T^2}+2|q|^2 q=0\,. \tag{8}$$

Analyzing and solving Eqs. (4)–(7), one can find a pair of *generic* compatibility conditions

$$\Gamma(z)=\alpha_r\frac{r_z(z)}{r(z)}+\alpha_d\frac{d_z(z)}{d(z)}+\alpha_p p(z)\,, \tag{9}$$

$$\Omega_2(z)=-\frac{d}{dz}\left[\frac{f_{rdp}(z)}{2d(z)}\right]+\frac{f_{rdp}^2(z)}{d(z)}, \tag{10}$$

where $\alpha_r = 1/4 - \lambda_r/2$, $\alpha_d = \lambda_d/2 - 1/4$, $g(z) = 2\alpha_p\int p(z)dz$ and $f_{rdp}(z) = (1/2-\alpha_r)r_z(z)/r(z)-(1/2+\alpha_d)d_z(z)/d(z)-\alpha_p p(z)$. The expressions for the self-similar solution variables are thus in the following forms:

$$A(z)=k_1\frac{r(z)^{(1-4\alpha_r)/2}}{d(z)^{(1+4\alpha_d)/2}}e^{-2\alpha_p\int p(z)dz}, \tag{11}$$

$$Z(z)=k_1^2\int\frac{r(z)^{2-4\alpha_r}}{d(z)^{1+4\alpha_d}}e^{-4\alpha_p\int p(z)dz}dz\,, \tag{12}$$

$$T(z,t)=k_1\frac{r(z)^{1-2\alpha_r}}{d(z)^{1+2\alpha_d}}e^{-2\alpha_p\int p(z)dz}t-2k_1\int\frac{r(z)^{1-2\alpha_r}}{d(z)^{2\alpha_d}}e^{-2\alpha_p\int p(z)dz}f_1(z)dz\,, \tag{13}$$

$$\varphi(z,t)=-\frac{f_{rdp}(z)}{2d(z)}t^2+f_1(z)t+f_2(z)\,, \tag{14}$$

$$f_1(z)=\frac{r(z)^{1-2\alpha_r}}{d(z)^{1+2\alpha_d}}e^{-2\alpha_p\int p(z)dz}\left[k_2+\int\Omega_1(z)\frac{d(z)^{1+2\alpha_d}}{r(z)^{1-2\alpha_r}}e^{2\alpha_p\int p(z)dz}dz\right], \tag{15}$$

$$f_2(z)=\int[-d(z)f_1^2(z)+\Omega_0(z)]dz\,, \tag{16}$$

where k_2 is a constant of integration determining the trajectory and phase of the similaritons. In compatibility conditions (9) and (10), α_p is an arbitrary real constant and $p(z)$ is an arbitrary matching function introduced to capture the residual gain/loss. The proposed *generic* self-similar transformation (2), in conjunction with Eq. (3), gives rise to *generic* compatibility conditions (9) and (10) and the set of self-similar solution variables (11)–(14). When combining Eq. (2) with Eqs. (11)–(16), Eq. (1) can be transformed into the standard NLS equation (8). Hence, we have established the connection between Eqs. (1) and (8). All known solutions to the latter—e.g., solitons [22], Akhmediev and Ma breathers (ABs and MBs, respectively) [23], and rogue waves (RWs) [24]—can now be mapped onto corresponding solutions of the former.

Note that compatibility conditions (9) and (10), along with the set of self-similar variables [see

Eqs. (11)–(14)], are closely tied to the free parameters α_r, α_d and α_p. Since those three constants are entirely arbitrary (including all positive and negative integers, rational and even irrational numbers), it follows that Eqs. (9) and (10) greatly relax the existence criteria of similaritons because the residual gain/loss function $p(z)$ is itself also arbitrary. When $\alpha_p = 0$, they predict an exact balance between gain/loss, dispersion and nonlinearity. However, when $\alpha_p \neq 0$, gain/loss cannot be completely compensated by dispersion and nonlinearity, and a residual gain/loss $p(z)$ survives. Since the choice of $p(z)$ is arbitrary, Eqs. (9) and (10) constitute weak constraints by compensating the unbalanced nature of dispersion, nonlinearity and gain/loss. Compared to those reported in earlier works [17, 18, 20, 29, 30, 32, 39-45] the introduction of arbitrary α_r, α_d, α_p and $p(z)$ necessarily results in a family of exact similariton solutions to Eq. (1) under *infinite* corresponding constraint conditions, which can take a diverse form of solutions. Especially, these constraint conditions are easier to realize in practice due to the introduction of free $p(z)$. In the next section, we will discuss the dynamic characteristics of the self-similar soliton (SS), self-similar AB (SAB), self-similar MB (SMB) and self-similar RW (SRW) solutions to Eq. (1) (explicit forms are given in Appendix A).

In accordance with Eqs. (14) and (15), the function $f_1(z)$ represents the frequency shift of similariton (2), and the width $W(z)$, trajectory $Tr(z)$, and the chirp $C(z)$ can also be derived from Eqs. (13) and (14) as follows:

$$W(z)=\frac{d(z)^{1+2\alpha_d}}{k_1 r(z)^{1-2\alpha_r}}e^{2\alpha_p\int p(z)dz}, \tag{17}$$

$$Tr(z)=2\frac{d(z)^{1+2\alpha_d}}{r(z)^{1-2\alpha_r}}e^{2\alpha_p\int p(z)dz}\int\frac{r(z)^{2-4\alpha_r}}{d(z)^{1+4\alpha_d}}\left[k_2+\int\Omega_1(z)\frac{d(z)^{1+2\alpha_d}}{r(z)^{1-2\alpha_r}}e^{2\alpha_p\int p(z)dz}dz\right]e^{-4\alpha_p\int p(z)dz}dz, \tag{18}$$

$$C(z)=\left(\alpha_r-\frac{1}{2}\right)\frac{r_z(z)}{r(z)d(z)}+\left(\frac{1}{2}+\alpha_d\right)\frac{d_z(z)}{d^2(z)}+\alpha_p\frac{p(z)}{d(z)}. \tag{19}$$

It is clear from inspection of Eqs. (15) and (17)–(19) that $f_1(z)$, $W(z)$, $Tr(z)$ and $C(z)$ are determined by the dispersion $d(z)$, nonlinearity $r(z)$ and matching function $p(z)$. Moreover, the trajectory and frequency shift are modulated by the linear external potential $\Omega_1(z)$. It is also worth emphasizing that the self-similar characteristic variables along with the self-similar transformation (2) are all associated with the free parameters α_r, α_d and α_p. Such connections imply that the different values of α_r, α_d and α_p may regulate the amplitude, effective propagation distance, width, the trajectory of the similaritons. Therefore, typical similaritons such as SSs, SABs, SMBs or SRWs are all fully

controllable and configurable. In order to better illustrate the significance of similariton solution (2), we make six important remarks.

Remark 1: **Amplitude.** The following deductions can be obtained from Eq. (11). When α_d = –1/4, it follows that $A(z) = k_1 r(z)^{1/2-2\alpha_r} e^{-2\alpha_p \int p(z)dz}$ and hence the amplitude of similariton (2) is not modulated by the dispersion $d(z)$. When α_r = 1/4, one has $A(z) = k_1 d(z)^{-1/2-2\alpha_d} e^{-2\alpha_p \int p(z)dz}$ and so the amplitude is not modulated by the nonlinearity $r(z)$. When $\alpha_r = -\alpha_d = 1/4$, we have $A(z) = k_1 e^{-2\alpha_p \int p(z)dz}$ so that the amplitude is independent of $r(z)$ and $d(z)$ [i.e., $A(z)$ changes exponentially with $p(z)$]. For the general case $\alpha_d \neq -1/4$ or $\alpha_r \neq 1/4$, the amplitude can be modulated in different ways even for the same $d(z)$ or $r(z)$.

Remark 2: **Effective distance.** The following deductions can be made from Eq. (12). When α_d = –1/4, one has $Z(z) = k_1^2 \int r(z)^{2-4\alpha_r} e^{-4\alpha_p \int p(z)dz} dz$ and so the effective distance is independent of $d(z)$. When $\alpha_r = 1/2$, one has $Z(z) = k_1^2 \int d(z)^{-1-4\alpha_d} e^{-4\alpha_p \int p(z)dz} dz$ so that the effective distance is independent of $r(z)$. When $\alpha_r = -2\alpha_d = 1/2$, one has $Z(z) = k_1^2 \int e^{-4\alpha_p \int p(z)dz} dz$ and hence the effective distance is independent of both $r(z)$ and $d(z)$ [i.e., $Z(z)$ depends only upon α_p and $p(z)$].

Remark 3: **Width.** The following deductions can be made from Eq. (17). When $\alpha_d = -1/2$, one has $W(z) = r(z)^{2\alpha_r - 1} e^{2\alpha_p \int p(z)dz} / k_1$ and so the width of similariton (2) is independent of the dispersion $d(z)$. When $\alpha_r = 1/2$, one has $W(z) = d(z)^{1+2\alpha_d} e^{2\alpha_p \int p(z)dz} / k_1$ and so the width is independent of $r(z)$. When $\alpha_r = -\alpha_d = 1/2$, the width depends only upon related to $p(z)$ and α_p. Furthermore, if $\alpha_p = 0$, the width of the similariton remains constant while, when $\alpha_d \neq -1/2$ and $\alpha_r \neq 1/2$, the width can be modulated by both $d(z)$ and $r(z)$ in different ways (as determined by the selection of α_d and α_r).

***Remark 4*: Trajectory.** If the system has no residual gain/loss (i.e., $\alpha_p = 0$), then for $\alpha_r = 1/2$ we have from Eq. (18) that $Tr(z) = 2d(z)^{1+2\alpha_d} \int d(z)^{-1-4\alpha_d} [k_2 + \int \Omega_1(z) d(z)^{1+2\alpha_d} dz] dz$. The trajectory of similariton (2) is then independent of $r(z)$. When $\Omega_1(z) \neq 0$, the trajectory is always related to the dispersion $d(z)$ regardless of α_d, which is in agreement with the propagation features found in Refs. [46, 47].

Remark 5: **Chirp.** For homogeneous system [where $d(z) = r(z) = 1$ and $p(z) = 0$], Eq. (19) predicts that similariton (2) is chirp-free. When $\alpha_r = 1/2$, one has $C(z) = (1/2 + \alpha_d) d_z(z)/d^2(z) + \alpha_p p(z)/d(z)$ so that the chirp of the similariton is independent of $r(z)$. In general, the similariton

always has a chirp related to $d(z)$ irrespective of α_d, except for the special cases of either $\alpha_r = -\alpha_d = 1/2$ and $\alpha_p = 0$, or $p(z) = (1/2 - \alpha_r)r_z(z)/[\alpha_p r(z)] - (1/2 + \alpha_d)d_z(z)/[\alpha_p d(z)]$.

Remark 6: **General cases.** From constraint (9), when the dispersion and nonlinearity are subject to the relation $d(z)^{\alpha_d} r(z)^{\alpha_r} = \text{const.}$, one has $\Gamma(z) = \alpha_p p(z)$ so that the matching function is determined solely by $\Gamma(z)$. Without loss of generality, we may always set const. = 1 and then deduce two special cases as important examples. Case ①: When $\alpha_r = -\alpha_d$ [i.e. $d(z) = r(z)$], it is known from Eqs. (11) and (17) that $A(z) = k_1 e^{-2\alpha_p \int p(z)dz}$ and $W(z) = k_1^{-1} e^{2\alpha_p \int p(z)dz}$. These results mean that both the amplitude and the width of similariton (2) are independent of $r(z)$ and $d(z)$, but they are dependent on $\Gamma(z)$. Case ②: When $\alpha_r = -2\alpha_d$ [i.e. $d(z) = r^2(z)$], one can obtain from Eq. (12) that $Z(z) = k_1^2 \int e^{-4\alpha_p \int p(z)dz} dz$ which means $Z(z)$ varies exponentially with $p(z)$ irrespective of $r(z)$ and $d(z)$.

From the above observations, it is easy to surmise that for an inhomogeneous system with given dispersion and nonlinearity, the similariton prescribed by Eqs. (2), (3) and (12)–(16) may have distinctly different qualitative behaviors whose amplitude, effective propagation distance, width, trajectory and chirp can all be controlled by choosing different α_r, α_d and α_p. In fact, the self-similar transformations reported in previous papers are some special cases of our work with particular choices of α_r, α_d and α_p [17, 18, 20, 29, 30, 39-45]. For example, when $\alpha_p = 0$, $5\alpha_d = 3\alpha_r$ and $r^5(z) = d^3(z)$, the constraint conditions and self-similar variables (9)–(16) can be reduced to those studied in Ref. [11]—as shown in Appendix B [see system (B1)]. When α_p, α_d and α_r take on other special values, the reduced expressions shown in Appendix B [see systems (B2)–(B4)] are in agreement with those in Refs. [12, 18, 33, 34]. Some special cases of self-similar transformation (2) are listed in Table 1, wherein "-" denotes that the nonlinearity or dispersion are homogeneous, and "*" signifies an arbitrary real constant. For homogeneous dispersion and nonlinearity, the values of α_r or α_d have no effect on constraint condition (9) due to $r_z(z)/r(z) = 0$ or $d_z(z)/d(z) = 0$. For ease of comparison, we note also that our $p(z)$ corresponds to the ratio $w_z(z)/w(z)$ in Refs. [32-34, 36].

The reported self-similar transformations listed in Table 1 are the special cases of our current work. The generality of similariton (2) arises from the introduction of arbitrary quantities α_r, α_d, α_p and $p(z)$. For homogeneous systems with $d(z) = 1/2$, $r(z) = 1$, $\Gamma(z) = -1/2$, $\Omega_0(z) = \Omega_1(z) = 0$ and $\Omega_2(z) = 1/2$, when $\alpha_r = \alpha_d = -2\alpha_p = 1$, the similariton (2) can reduce to the similar but a little bit different

with the one in Ref. [1] due to unidentical self-similar transformations. For inhomogeneous systems, the constraints imposed by Eqs. (9) and (10) are easy to satisfy and the corresponding similaritons can be diversely regulated by choosing different values of α_r, α_d, α_p and $p(z)$ at will. Without loss of generality, in the subsequent sections we demonstrate the dynamics of similaritons with different free parameters in periodic nonlinear systems.

Table 1 Some special cases of the self-similar transformation (2)

References	α_p	α_r	α_d
Refs. [20, 29, 30, 39-41]	0	0	0
Refs. [15-17, 32, 42-45]	0	0	-
Ref. [11]	0	α_r	$0.6\alpha_r$
Ref. [18]	0	0	–1/2
Ref. [18]	0	1/2	–1
Refs. [12, 18]	0	1/2	–1/2
Ref. [35]	0	1/4	-
Ref. [32]	1/2	1/2	–1/2
Ref. [36]	1/2	1/2	-
Refs. [33, 34]	1/2	-	-
This work	*	*	*

3. Dynamics of similaritons in inhomogeneous nonlinear systems

It has been demonstrated above that the dynamics of similaritons can be modulated by free parameters α_r, α_d and α_p. For simplicity, here we investigate only the role of α_r by setting $\alpha_p = 0$ and considering a simple inhomogeneous nonlinear system [18, 40]:

$$r(z) = 1 + \varepsilon \cos(2z), \quad d(z) = 1, \tag{20}$$

where ε is the fluctuation parameter of $r(z)$ and we set $\varepsilon = 1/2$ for definiteness. Since $d_z(z)/d(z) = 0$, α_d does not affect constraint conditions (9) and (10) or similariton solution (2). Recall that the potential $\Omega_0(z)$ influences only the phase and the potential $\Omega_1(z)$ changes the trajectory and frequency shift [18, 39]. Hence, in the subsequent analysis, we set $\Omega_0(z) = \Omega_1(z) = 0$ and the constant $k_1 = 1$ in order to isolate the role of α_r.

In accordance with Eqs. (9)–(12), the system parameters $I(z)$, $\Omega_2(z)$ and self-similar variables $A(z)$ and $Z(z)$ will take the simple forms following from system (20):

$$I'(z) = -2\alpha_r \sin(2z)/[2 + \cos(2z)], \tag{21}$$

$$\Omega_2(z) = (1 - 2\alpha_r)\frac{3 - 2\alpha_r + 4\cos(2z) + (2\alpha_r - 1)\cos(4z)}{2[2 + \cos(2z)]^2}, \tag{22}$$

$$A(z) = [1+\cos(2z)/2]^{1/2-2\alpha_r}\ , \tag{23}$$

$$Z(z) = \int [1+\cos(2z)/2]^{2-4\alpha_r}\, dz\,. \tag{24}$$

For different values of α_r, the specific forms of $\Gamma(z)$, $\Omega_2(z)$, $A(z)$ and $Z(z)$ in Eqs. (21)–(24) evidently change significantly. Figure 1 depicts their profiles when α_r = 1/4, 1/2 and –3/2, respectively. It can be seen that $\Gamma(z)$ has the same period but different amplitudes and slopes for those choices of α_r. The parabolic potential $\Omega_2(z)$ has the same period with different shapes for α_r = 1/4 and –3/2, but its periodicity vanishes for α_r = 1/2. The amplitude $A(z)$ is constant for α_r = 1/4, while for α_r = 1/2 and –3/2 it has complementary peaks and troughs at the same fixed period. The depth of modulation in $A(z)$ is also much greater for α_r = –3/2 than for α_r = 1/2. Finally, the effective propagation distance $Z(z)$ takes periodic oscillation, linear and step-like forms, respectively.

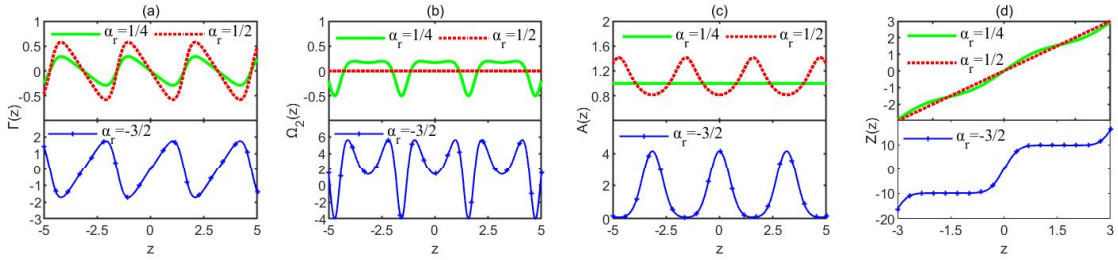

Fig. 1. The profiles of (a) $\Gamma(z)$, (b) $\Omega_2(z)$, (c) $A(z)$ and (d) $Z(z)$ for α_r = 1/4, 1/2 and –3/2 in inhomogeneous nonlinear system (20).

From the similariton solutions (given in Appendix A), it is straightforward to find specific expressions for the SS, SAB, SMB and SRW with α_r = 1/4, 1/2, –3/2 in inhomogeneous nonlinear system (20); evolutions of those waves are shown in Fig. 2. When α_r = 1/4 and –3/2, the trajectories of the SS, SMB and SRW oscillate periodically; their peak intensities and background fields are unmodulated when α_r = 1/4 [see Figs. 2(a_1)–(d_1)] but they exhibit periodic oscillations when α_r = –3/2 [see Figs. 2(a_3)–(d_3)]. The SS is an exception since its background field is necessarily zero [see Fig. 2(a_3)], as predicted by Eqs. (23), (17) and (18). When α_r = 1/2, the intensities and backgrounds of the similaritons oscillate periodically except for the background of the SS, and due to $Tr(z) = 2k_2z$, their trajectories vary linearly in the (z,t) plane [see Figs. 2(a_2)–(d_2)]. It is worth noting that when α_r = –3/2, a very high-intensity pulse train and pulse can be generated [see Figs. 2(b_3)–(d_3)].

According to Eq. (18), the trajectories of the similaritons are prescribed by $Tr(z) = 2k_2[1 + \varepsilon\cos(2z)]^{-1/2}[z + \varepsilon\sin(2z)/2]$, $2k_2z$ and $2k_2[1 + \varepsilon\cos(2z)]^{-4}\int[1 + \varepsilon\cos(2z)]^8 dz$, when α_r = 1/4, 1/2 and –3/2. It follows that the peaks of the SS, SAB, SMB and SRW are tilted when α_r = 1/2 and skewed

when α_r = 1/4, –3/2 [where the trajectories may be linear or curved in the (z,t) plane, respectively].

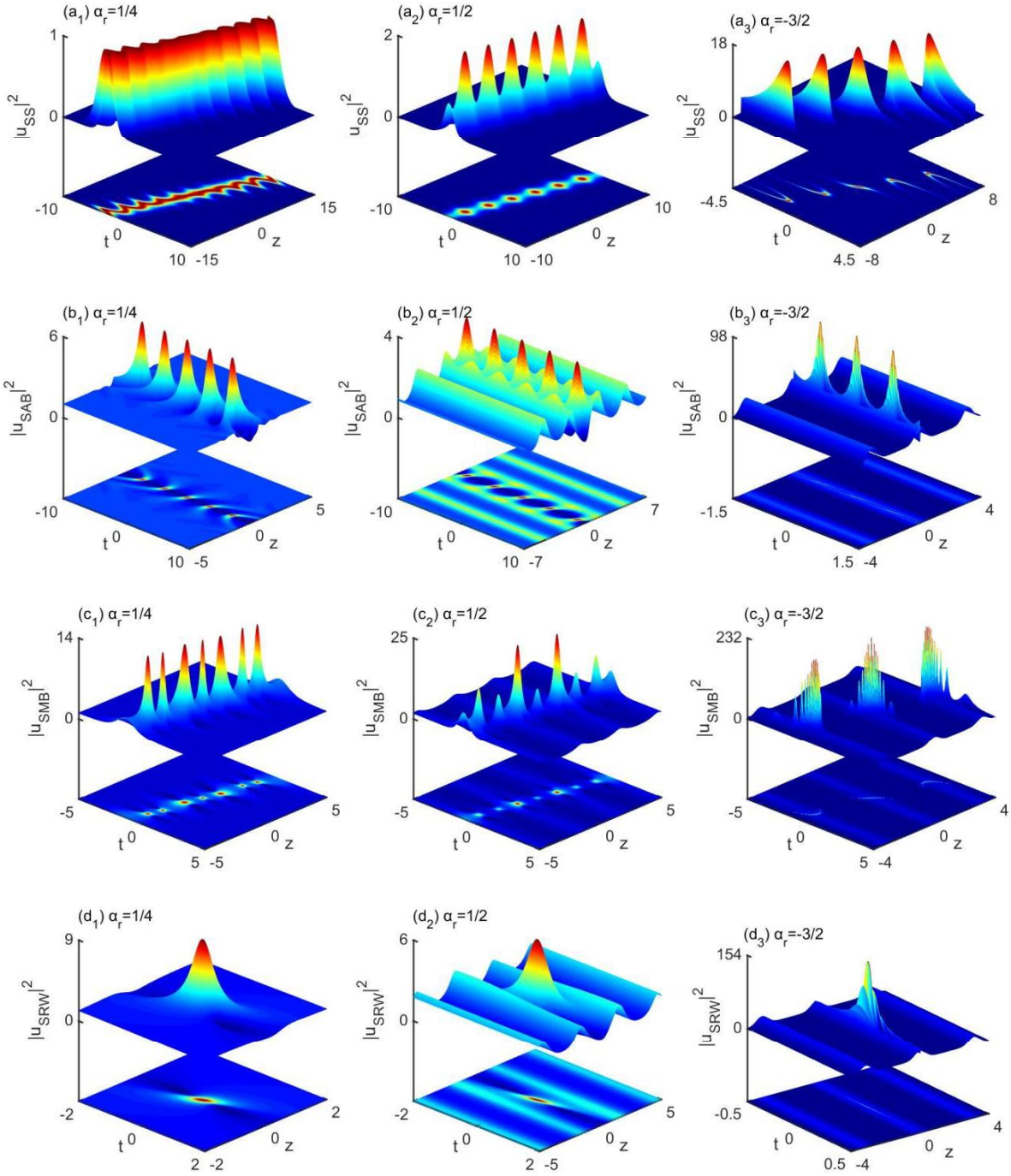

Fig.2. Evolution of (a) the SS (A1) with η_s = 1, δ_s = 0, φ_s = 0, T_s = 0, k_2 = 0.1; (b) the SAB (A2) with ω_{ab} = 0.8, T_{ab} = 0, Z_{ab} = 0, k_2 = 0.5; (c) the SMB (A3) with ω_m = 0.8, T_m = 0, Z_m = 0, k_2 = 0.1; (d) the SRW (A4) with α_g = 1, T_g = 0, Z_g = 0, k_2 = 0.5, in the system (20) for different α_r, respectively. The other parameters are the same as in Fig. 1.

It is worth reemphasizing that the similariton properties discussed above are strictly for α_p = 0. For $\alpha_p \neq 0$, Eqs. (9) –(16) predict that the residual gain/loss $p(z)$ is not only related to the constraint conditions, but it also affects the similariton parameters. In order to explore the role of $p(z)$, here we

set $\varepsilon = 0$ in system (20) [i.e., so that $r(z) = 1 = d(z)$]. Thereafter, the parabolic potential $\Omega_2(z)$, the self-similar amplitude $A(z)$ and the effective propagation distance $Z(z)$ take the forms of: $\Omega_2(z) = \alpha_p[p_z(z) + 2\alpha_p p^2(z)]/2$, $A(z) = \exp(-2\alpha_p \int p(z)dz)$ and $Z(z) = \int[\exp(-4\alpha_p \int p(z)dz)]dz$. These functions evidently depend strongly upon $p(z)$. Figure 3 shows the profiles of $\Omega_2(z)$, $A(z)$ and $Z(z)$ for periodic $p(z) = -\sigma_p\rho_p \sin(\rho_p z)/[1 + \sigma_p \cos(\rho_p z)]$ [27] and linear $p(z) = \varepsilon_p z$ [7], respectively, where it can be seen that $\Omega_2(z)$, $A(z)$ and $Z(z)$ have very different profiles for these two choices. For periodic $p(z)$, the functions $\Omega_2(z)$, $A(z)$ and $Z(z)$ all have the same period as that of $p(z)$ [see Fig. 3(a)]; for linear $p(z)$, we find $\Omega_2(z)$ has a parabolic profile, $A(z)$ goes to zero at $z \to \pm\infty$, and $Z(z)$ is of kink form [see Fig. 3(b)]. These results demonstrate that $p(z)$, when unbalanced by the nonlinearity and dispersion, not only relaxes the existence conditions for similaritons but it can also control the amplitude and evolution of such waves.

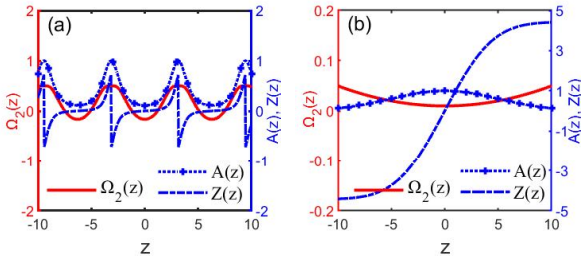

Fig. 3. The profiles of $\Omega_2(z)$, $A(z)$ and $Z(z)$ in the system (20) with $\varepsilon = 0$, (a) $p(z) = -\sigma_p \rho_p \sin(\rho_p z)/[1 + \sigma_p \cos(\rho_p z)]$ and (b) $p(z) = \varepsilon_p z$, where $\rho_p = 1$, $\sigma_p = 0.5$ $\varepsilon_p = 0.1$ and $\alpha_p = 1$.

Evolution of the SS, SAB, SMB and SRW for the periodic and linear $p(z)$ are presented in Fig. 4. In the periodic case [see Figs. 4(a_1)–4(d_1)], all four solutions either oscillate periodically or repeat along the propagation direction due to the form of the function

$$Z(z) = k_1^2 \left(\frac{22 \arctan[\tan(z/2)/\sqrt{3}]}{27\sqrt{3}} - \frac{\sin(z)}{9[2+\cos(z)]^3} - \frac{5\sin(z)}{27[2+\cos(z)]^2} - \frac{8\sin(z)}{27[2+\cos(z)]} \right).$$

The periodic nature of the SS [see Fig. 4(a_1)] is different from that shown in Figs. 2(a_2) and 2(a_3), the peaks of the SAB are temporally 'bent' to two sides [see Fig. 4(b_1)], and the SMB and SRW appear, respectively, as a spatially-localized three-hump [see Fig. 4 (c_1)] and double-hump waves [see Fig. 4(d_1)]. In the linear case, the evolution of the SS and SMB [see Figs. 4(a_2) and 4(c_2), respectively] are spatially localized on a zero-background due to $A(z) = \exp(-\alpha_p \varepsilon_p z^2)$; they are qualitatively different from the solutions shown in Figs. 2(a) and 2(c), and also from those

appearing in the literature [6, 20]. Finally, the SAB retains spatial localization while the SRW exhibits both spatial and temporal localization; both waves exist on a zero-background [see Figs. 4(b_2) and 4(d_2)], which is again different from the conventional AB and RW [7, 28].

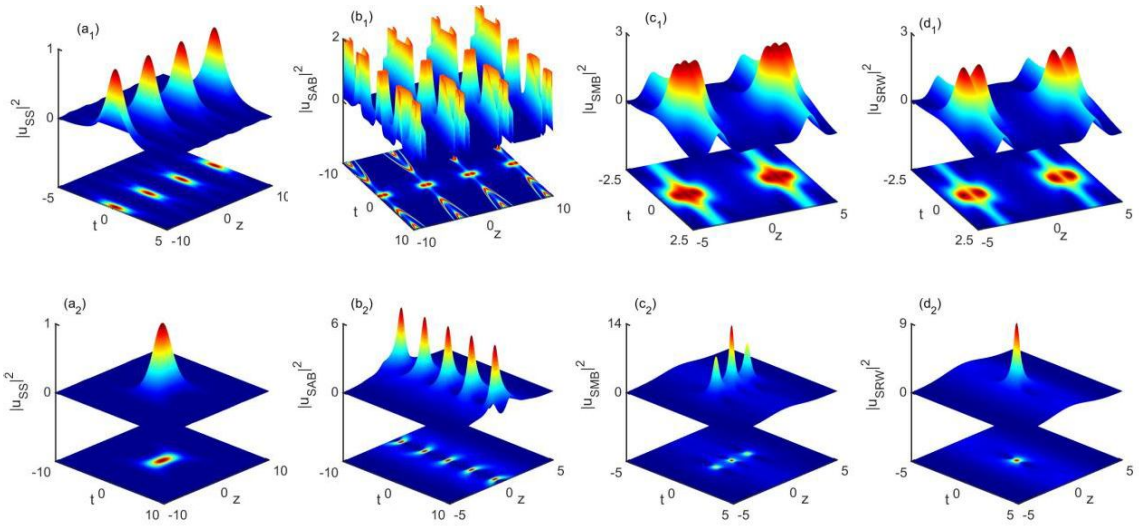

Fig.4. Evolution of the (a) SS, (b) SAB, (c) SMB and (d) SRW in system (20) with periodic (top row) and linear (bottom row) $p(z)$. The corresponding parameters are the same as in Fig. 3.

4. Diversely composite waves in coherently coupled inNLS model

As a direct application of the new similariton solutions, we now consider a coupled inNLS model that captures the phenomenon of four-wave mixing [17, 18] :

$$\begin{aligned} &i\frac{\partial Q_1}{\partial z}+d(z)\frac{\partial^2 Q_1}{\partial t^2}+2r(z)(|Q_1|^2+2|Q_2|^2)Q_1+2r(z)Q_2^2Q_1^*+V(z,t)Q_1+i\Gamma(z)Q_1=0,\\ &i\frac{\partial Q_2}{\partial z}+d(z)\frac{\partial^2 Q_2}{\partial t^2}+2r(z)(|Q_2|^2+2|Q_1|^2)Q_2+2r(z)Q_1^2Q_2^*+V(z,t)Q_2+i\Gamma(z)Q_2=0, \end{aligned} \tag{25}$$

where $V(z, t)$ is the same here as in Section 3. In order to solve these coupled equations, we substitute the linear transformation [17, 18] for Q_1 and Q_2:

$$Q_j(z,t)=\frac{q_1(z,t)-(-1)^j q_2(z,t)}{2},\ j=1,2, \tag{26}$$

into system (25). That procedure generates a new pair of independent (i.e., decoupled) equations of the inNLS type, namely

$$i\frac{\partial q_j}{\partial z}+d(z)\frac{\partial^2 q_j}{\partial t^2}+2r(z)|q_j|^2 q_j+V(z,t)q_j+i\Gamma(z)q_j=0,\ j=1,2\,. \tag{27}$$

Since Eq. (27) has the same form as Eq. (1), its solutions such as SS, SAB, SMB and SRW can be

deployed with the aid of Eq. (26) to construct composite waves that satisfy system (25). For convenience henceforth, we define the symbol "X–Y" to denote such solutions which are combinations of self-similar solutions X and Y of Eq. (27) (e.g., "SAB–SMB" denotes a composite wave composed of an SAB and an SMB).

We continue with periodic nonlinear system (20) and apply the explicit self-similar solutions (A1)–(A4) of Eq. (1) to study the propagation of composite waves of system (25). As before, the parameter α_d plays no role in the problem since $d_z(z)/d(z)=0$. Thus, it is necessary to investigate only the effect of varying α_r. The evolution of the two components for typical composite waves is shown in Fig. 5. When $\alpha_r = 1/4$, the trajectories of the SS–SS change periodically with z, while the intensities of two components remain unchanged [except for a peak appearing in $|Q_1|^2$ and a valley in $|Q_2|^2$ at the collision point—see Figs. 5(a_1), 5(a_2), respectively]. When $\alpha_r = 1/2$, the trajectories of the two components of the SS–SS wave are unmodulated by the periodic nonlinearity while the intensities fluctuate periodically as the waves undergo an energy exchange process [appearing as two peaks in $|Q_1|^2$, or a valley in $|Q_2|^2$ at the collision point—see Figs. 5(b_1) and 5(b_2), respectively]. These properties are fully consistent with the expressions for the amplitude [Eq. (3)] and trajectory [Eq. (18)], where the $A(z)$ is a constant for $\alpha_r = 1/4$ and $Tr(z)$ is a constant for $\alpha_r = 1/2$.

Figures 5(c) and 5(d) also shows the evolution of the SAB–SMB intensity with $\alpha_r = 1/4$ and 1/2, respectively. The background waves of both components with $\alpha_r = 1/2$ exhibit periodic fluctuations [see Fig. 5(d)], while those with $\alpha_r = 1/4$ do not [see Fig. 5(c)]. A further observation is that the intensities of the background waves in both cases change abruptly at the location (T_m, Z_{ab}) of the collision between the SAB and SMB waves.

Figures 5(e) and 5(f) plot the intensities of SRW–SRW components with $\alpha_r = 1/4$ and 1/2, respectively. When $\alpha_r = 1/4$, we find $|Q_1|^2$ appears to be 'volcano-shaped' [as per a classic RW-like solution – see Fig. 5(e_1)]. In contrast, when $\alpha_r = 1/2$, we find $|Q_1|^2$ has the form of a 'volcano'-shaped distribution on a strongly fluctuating background wave [see Fig. 5(f_1)]. It is interesting to note that $|Q_2|^2$ for both values of α_r present a localized bimodal structure on zero-amplitude background [see Figs. 5(e_2) and 5(f_2)]. Such states may be used to generate high-power twin pulses localized in space-time.

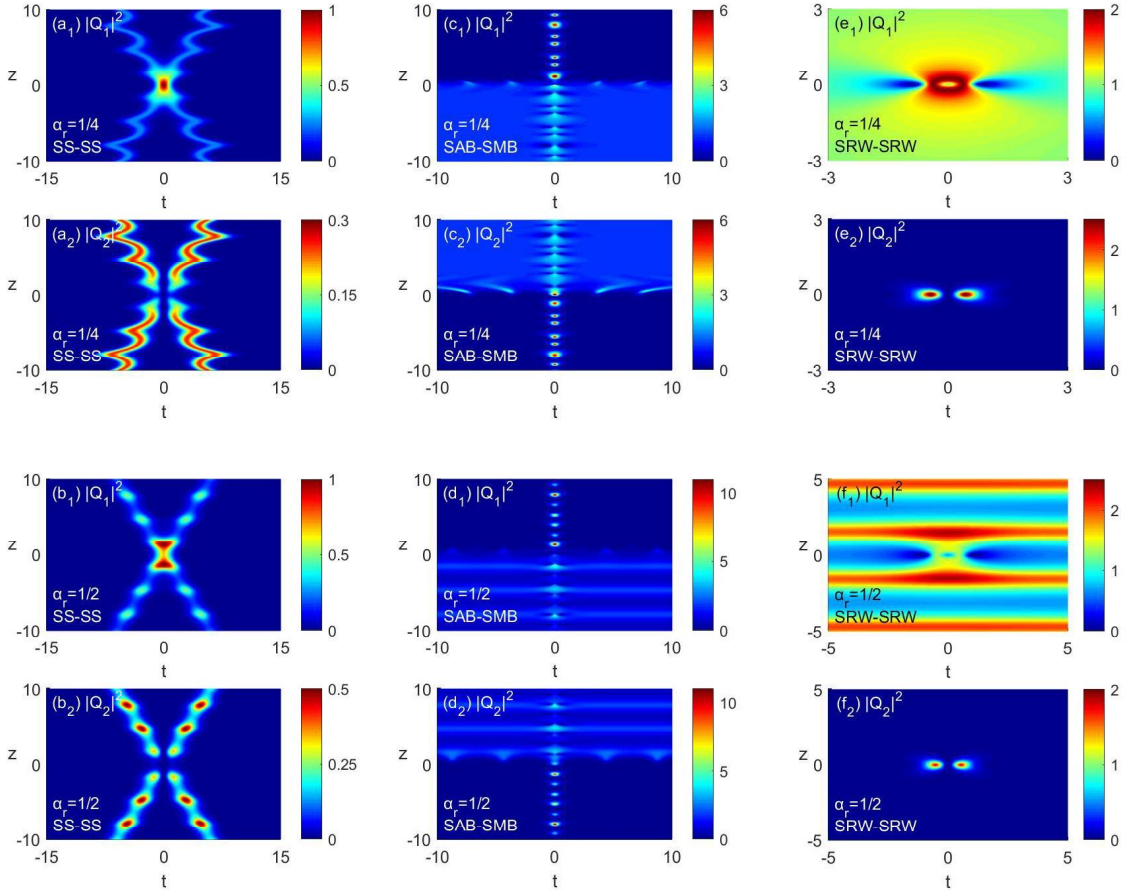

Fig. 5. Intensity evolution of typical composite waves in periodic nonlinear system (20) for $\alpha_r = 1/4$ (top two rows) and $\alpha_r = 1/2$ (bottom two rows), respectively. (a, b) The SS–SS with $\eta_{s1} = \eta_{s2} = 1$, $\delta_{s1} = -\delta_{s2} = 0.3$, $\varphi_{s1} = \varphi_{s2} = 0$, $T_{s1} = T_{s2} = 0$, (c, d) the SAB–SMB with $\omega_{ab} = 0.8$, $T_{ab} = 0$, $Z_{ab} = 0.6$; $\omega_m = 0.8$, $T_m = 0$, $Z_m = 0$; and (e, f) the SRW-SRW with $\alpha_{g1} = \alpha_{g2} = 1$, $T_{g1} = -T_{g2} = 0.5$, $Z_{g1} = Z_{g2} = 0$. The other parameters are the same as in Fig.1.

To emphasize the central role of $p(z)$, we consider the special case of $\varepsilon = 0$ in the system (20) and choose periodic or linear forms according to $p(z) = -\sigma_p \wp_p \sin(\wp_p z)/[1 + \sigma_p \cos(\wp_p z)]$ and $p(z) = \varepsilon_p z$, respectively. The evolution of the corresponding SS–SS, SAB–SMB and SRW–SRW are presented in Fig. 6. It is evident that the two different choices of $p(z)$ can have a strong impact on the qualitative properties and controllable features of the composite waves; in particular, we naturally see more varied qualitative phenomena for the coupled-inNLS model than for the inNLS model. With the periodic $p(z)$, intensity $|Q_1|^2$ of the SS–SS composite wave comprises a zero-background RW-like state while $|Q_2|^2$ behaves as 'eyes-like' waves at periodic collision positions [due to the periodic modulation by $p(z)$ and $\Omega_2(z)$—see Figs. 6(a_1) and 6(a_2), respectively]. With the linear $p(z)$, both $|Q_1|^2$ and $|Q_2|^2$ of the SS–SS are spatially and temporally localized, where $|Q_1|^2$ has a nonperiodic zero-background RW-like state and $|Q_2|^2$ is a nonperiodic 'butterfly-like' wave [due to

the modulations by $p(z)$ and $\Omega_2(z)$—see Figs. 6(b_1) and 6(b_2), respectively].

Comparing Figs. 6(c) and 6(d), we see that the SAB component of the SAB–SMB composite wave is much stronger in $|Q_2|^2$ than in $|Q_1|^2$. The peaks of the SAB components are 'bent' to two sides around the collision points in both $|Q_1|^2$ and $|Q_2|^2$, while the SMB components manifest single-hump [see Fig. 6(c_2)], double-hump [see Figs. 6(c_1) and 6(d_2)] and triple-hump [see Fig. 6(d_1)] structures, except for periodicity of the composite wave in Figs. 6(c) for periodic $p(z)$.

Figures 6(e) and 6(f) show the evolution of SRW–SRW composite waves. For periodic $p(z)$, intensity $|Q_1|^2$ appears to be periodic RW-like with bright wings [cf. Fig. 5(e_1)] while $|Q_2|^2$ has a periodic 'butterfly'-shaped structure [see Fig. 6(e_2)]. For linear $p(z)$, a 'volcano'-shaped RW-like structure appears in $|Q_1|^2$ [see Fig. 6(f_1)] while twin RW-like structures appear in $|Q_2|^2$ [see Fig. 6(f_2)].

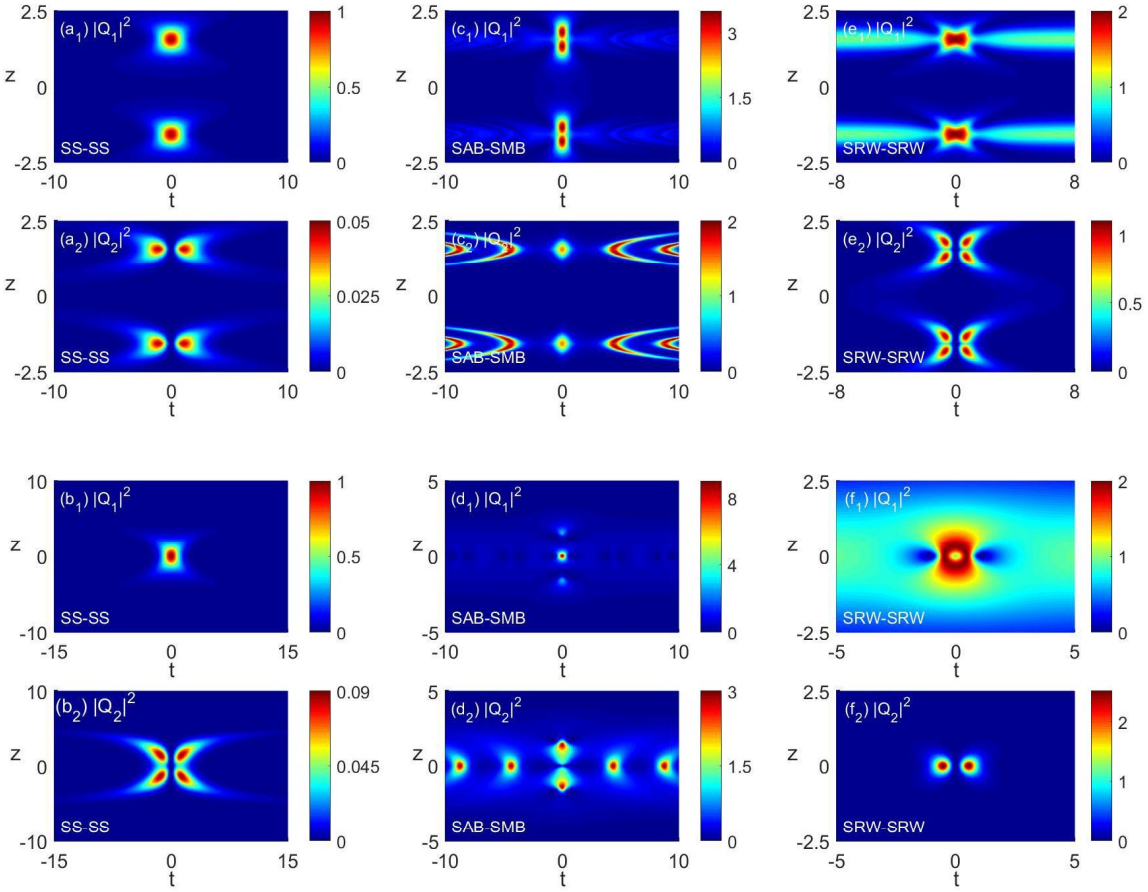

Fig. 6. Evolution of the (a, b) SS-SS, (c, d) SAB-SMB and (e, f) SRW-SRW in the coupled system with periodic (top two rows) and linear (bottom two rows) $p(z)$, respectively. The parameters of SS, SAB, SMA SRW are the same as in Fig. 5 except for $Z_{ab} = 0$. The parameters of $p(z)$ are the same as in Fig. 3(a) and 3(b), respectively.

Finally, we investigate the evolution of composite waves SS–SAB, SAB–SRW, and SMA–SRW [see Fig. 7] by choosing the same forms of $p(z)$ and inhomogeneous systems as those in Fig. 6. After comparing Figs. 7 (a), 7(c), and 7(e), and also Figs. 7(b), 7(d), and 7(f), one can observe diverse waveforms and collision points of the SAB(SRW) component due to different component nonlinear dynamics. On the one hand, periodic single-hump [see Figs. 7 (a_1), 7(c_2), 7(e_2)] and double-hump [see Figs. 7 (a_2), 7(c_1), 7(e_1)] structures appear for the periodic $p(z)$. On the other hand, valley [see Figs. 7 (d_2)], single-hump [see Figs. 7(b_2), 7(d_1), 7(f_1)], and double-hump [see Figs. 7 7(b_1), 7(f_2)] structures are manifest for linear $p(z)$. The peaks of the SAB component of the SS–SAB composite wave are 'bent' to two sides around the collision points in both $|Q_1|^2$ and $|Q_2|^2$ [see Figs. 7(a)–7(d)]. Two evolutions of SMA–SRW composite waves are shown in Figs. 7(e) and 7(f). For periodic $p(z)$, the intensity $|Q_1|^2$ appears to be a periodic double-RW-like structure with bright wings [cf. Fig. 7(e_1)] while $|Q_2|^2$ has a periodic 'rugby ball'-shaped structure [see Fig. 7(e_2)]. For linear $p(z)$, a RW-like structure with six dark holes appears in $|Q_1|^2$ [see Fig. 7(f_1)] while twin RW-like structures appear in $|Q_2|^2$ along the z axis [cf. Fig. 7(f_2)]. Such abundant properties imply that one can achieve diversely controllable composite waves through careful design of the gain/loss and potential distributions.

5. Conclusions

In this work, we have reported a family of exact similariton solutions for an inNLS equation with external potentials by proposing a generic self-similar transformation and identifying relaxed constraint conditions that combine gain/loss, dispersion, nonlinearity, and a matching function representing residual gain/loss. The parameters involved in the constraint conditions can be arbitrary real constants, implying that: (i) the existence condition of the similaritons can be relaxed, and (ii) there exists an infinite number of similariton solutions that can be readily controlled with a careful choice of parameters. Taking a nonlinear inhomogeneous system with periodic properties, we uncovered rich dynamical behaviors associated with propagating similaritons. Furthermore, we applied these newly-derived similariton solutions to a pair of coupled inNLS equations which included four-wave mixing terms. This procedure has allowed to investigate, for the first time, families of diversely controllable composite waves such as SS–SS, SAB–SMB and SRW–SRW.

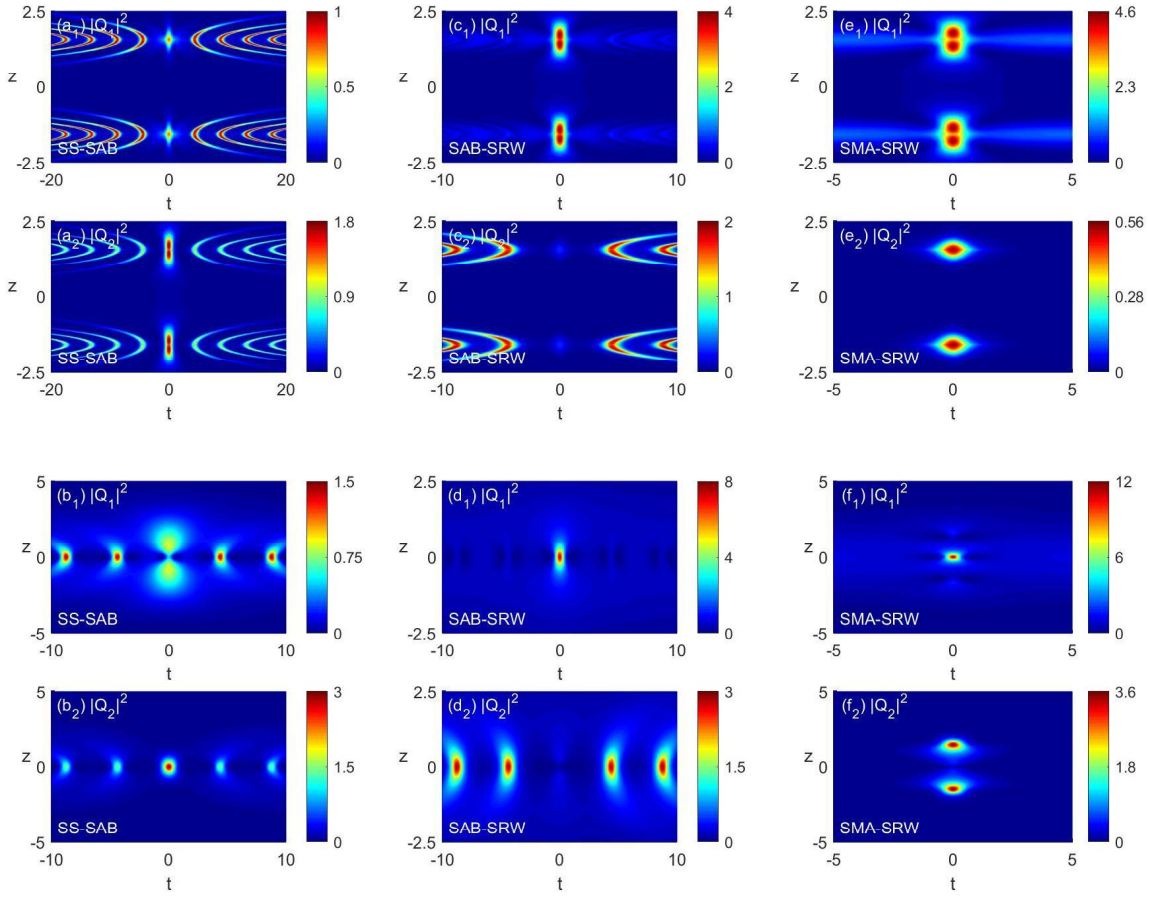

Fig. 7. Evolution of the (a, b) SS-SAB, (c, d) SAB-SRW and (e, f) SMA-SRW in the coupled system with periodic (top two rows) and linear (bottom two rows) $p(z)$, respectively. The other parameters of the SS, SAB, SRW and SMA are the same as in Fig. 6 except for δ_s =0, Z_{ab} = 0, T_g = 0. The periodic and linear parameters of $p(z)$ are the same as in Fig. 3(a) and (b), respectively.

It should be pointed out that the foregoing analysis is only in the designated systems with different free parameters α_r, α_d and α_p or $p(z)$ as examples, which can achieve plentifully modulated self-similar waves. In fact, the exact similaritons family presented in this work suggest a more in-depth study into the dynamics of single- and two-component similaritons over a much greater range of their non-trivial parameter spaces. Investigating other systems and parameter regimes may provide further insight into designing inhomogeneous fibers in order to realize special wave control and transmission.

In addition, Eq. (8) is a classic nonlinear physical model for wave envelopes which has abundant exact solutions, including N-soliton solutions, first-order and higher-order breathers and RW solutions [25, 26, 48]. By deploying other known solutions of Eq. (8) in combination with transformations (2) and (25), one can uncover a much wider range of evolution characteristics and

modulation mechanisms relating to more exotic composite waves in coupled inNLS systems.

Appendix A: Explicit Self-Similar Solutions of Eq. (1)

The explicit solutions of SS, SAB, SMB and SRW for inNLS Eq. (1) can be obtained by combining Eqs. (11)–(16) and the exact solutions of the soliton [22], Akhmediev and Ma breather [23], and rogue wave (RW) [24] of Eq. (8), which are expressed as follows:

(1) Exact SS solution:

$$u_{SS}=k_1\eta_s\frac{r(z)^{(1-4\alpha_r)/2}}{d(z)^{(1+4\alpha_d)/2}}\mathrm{sech}[\eta_s(T-T_s+2\delta_s Z)]e^{i[(\eta_s^2-\delta_s^2)Z-\delta_s T+\varphi_s+\varphi(z,t)]-2\alpha_p\int p(z)dz}, \tag{A1}$$

where η_s, δ_s, T_s and φ_s represent the amplitude, frequency, initial position and phase of the SS, respectively.

(2) Exact SAB solution

$$u_{SAB}=k_1\frac{r(z)^{(1-4\alpha_r)/2}}{d(z)^{(1+4\alpha_d)/2}}\frac{\cosh[a(Z-Z_{ab})-2i\omega_{ab}]-\cos(\omega_{ab})\cos[b(T-T_{ab})]}{\cosh[a(Z-Z_{ab})]-\cos(\omega_{ab})\cos[b(T-T_{ab})]}\times e^{i[2(Z-Z_{ab})+\varphi(z,t)]-2\alpha_p\int p(z)dz}, \tag{A2}$$

where a = 2sin(2ω_{ab}), b = 2sin(ω_{ab}), $\omega_{ab}\in\mathbb{R}$. The parameters Z_{ab} and T_{ab} are, respectively, related to the initial position and time-shift of the SAB.

(3) Exact SMB solution

$$u_{SMB}=k_1\frac{r(z)^{(1-4\alpha_r)/2}}{d(z)^{(1+4\alpha_d)/2}}\frac{\cos[m_a(Z-Z_m)-2i\omega_m]-\cosh(\omega_m)\cosh[m_b(T-T_m)]}{\cos[m_a(Z-Z_m)]-\cosh(\omega_m)\cosh[m_b(T-T_m)]}\times e^{i[2(Z-Z_m)+\varphi(z,t)]-2\alpha_p\int p(z)dz}, \tag{A3}$$

where m_a = 2sinh(2ω_m), m_b = 2sinh(ω_m), $\omega_m\in\mathbb{R}$. The parameters Z_m and T_m determine the initial position and time-shift of the SMB, respectively.

(4) Exact SRW solution

$$u_{SRW}=k_1\frac{r(z)^{(1-4\alpha_r)/2}}{d(z)^{(1+4\alpha_d)/2}}\alpha_g\left[1-\frac{4+i16|\alpha_g|^2(Z-Z_g)}{1+4|\alpha_g|^2(T-T_g)+16|\alpha_g|^4(Z-Z_g)^2}\right]e^{i\left[2|\alpha_g|^2(Z-Z_g)+\varphi(z,t)\right]-2\alpha_p\int p(z)dz}, \tag{A4}$$

where α_g is related to the background intensity of the SRW. The parameters Z_g and T_g determine the initial position and time-shift of the SRW, respectively. Here, the self-similar variables $Z\equiv Z(z)$ and $T\equiv T(z,t)$ in (A1)–(A4) are given by Eqs. (12) and (13), respectively.

Appendix B: Some Special Cases of Similariton (2)

(1) When $\alpha_p = 0$, $5\alpha_d = -3\alpha_r$, $r^5(z) = d^3(z)$ and $\Omega_0 = 0$, under the constraint conditions $\Gamma(z) = 0$ and $\Omega_2(z) = [-8d_z^2(z) + 5d(z)d_{zz}(z)] /[50d^3(z)]$, the self-similar variables are reduced to those studied in Ref. [11] :

$$A(z) = k_1 d^{-1/5}(z), \tag{B1.1}$$

$$Z(z) = k_1^2 \int d^{1/5}(z)dz, \tag{B1.2}$$

$$T(z,t) = k_1 d^{-2/5}(z)t - 2k_1 \int d^{1/5}(z)\left(k_2 + \int d^{2/5}(z)\Omega_1(z)dz\right)dz, \tag{B1.3}$$

$$\varphi(z,t) = \frac{d_z(z)}{10d^2(z)}t^2 + \frac{\int d^{2/5}(z)\Omega_1(z)dz}{d^{2/5}(z)}t - \int d^{1/5}(z)\left(k_2 + \int d^{2/5}(z)\Omega_1(z)dz\right)^2 dz. \tag{B1.4}$$

(2) When $\alpha_p = 0$, $\alpha_r = 0$, $\alpha_d = -1/2$ and $\Omega_0(z) = 0$, under the constraint conditions $\Gamma(z) = -d_z(z)/2d(z)$ and $\Omega_2(z) = [r(z)r_z(z)d_z(z) + 2d(z)r_z^2(z) - d(z)r(z)r_{zz}(z)$, the self-similar variables are reduced to the first case reported in Ref. [18]:

$$A(z) = k_1\left[d(z)r(z)\right]^{1/2}, \tag{B2.1}$$

$$Z(z) = k_1^2 \int d(z)r^2(z)dz, \tag{B2.2}$$

$$T(z,t) = k_1 r(z)t - 2k_1 \int \left[d(z)r^2(z)\left(k_2 + \int \frac{\Omega_1(z)}{r(z)}dz\right)\right]dz, \tag{B2.3}$$

$$\varphi(z,t) = -\frac{r_z(z)}{4d(z)r(z)}t^2 + r(z)\left[k_2 + \int \frac{\Omega_1(z)}{r(z)}dz\right]t - \int \left[d(z)r^2(z)\left(k_2 + \int \frac{\Omega_1(z)}{r(z)}dz\right)^2\right]dz. \tag{B2.4}$$

(3) When $\alpha_p = 0$, $\alpha_r = 1/2$, $\alpha_d = -1/2$ and $\Omega_0(z) = 0$, under the constraint conditions $\Omega_2(z) = 0$ and $\Gamma(z) = r_z(z)/2r(z) - d_z(z)/2d(z)$, the self-similar variables are reduced to those reported in Refs. [12, 18]:

$$A(z) = k_1\left[d(z)/r(z)\right]^{1/2}, \tag{B3.1}$$

$$Z(z) = k_1^2 \int d(z)dz, \tag{B3.2}$$

$$T(z,t) = k_1 t - 2k_1 \int d(z)\left(k_2 + \int \Omega_1(z)dz\right)dz, \tag{B3.3}$$

$$\varphi(z,t) = [k_2 + \int \Omega_1(z)dz]t - \int [d(z)(k_2 + \int \Omega_1(z))^2]dz. \tag{B3.4}$$

(4) When $\alpha_p = 1/2$, $\alpha_r = 0$, $\alpha_d = 0$, $p(z) = w_z(z)/w(z)$ and $d(z) = r(z) = 1$, $\Omega_0(z) = \Omega_1(z) = 0$, under the constraint conditions $\Gamma(z) = w_z(z)/2w(z)$ and $\Omega_2(z) = w_{zz}(z)/4w(z)$,, the self-similar variables are reduced to those reported in Refs. [33, 34]:

$$A(z)=\frac{k_1}{w(z)}, \tag{B4.1}$$

$$Z(z)=k_1^2\int w^{-2}(z)dz, \tag{B4.2}$$

$$T(z,t)=k_1w^{-1}(z)t-2k_1k_2\int w^{-2}(z)dz, \tag{B4.3}$$

$$\varphi(z,t)=\frac{w_z(z)}{4w(z)}t^2+\frac{k_2}{w(z)}t-k_2^2\int\frac{1}{w^2(z)}dz. \tag{B4.4}$$

It should be pointed out that there is a slight difference among Appendix B and Refs. [11, 12, 18, 33, 34] due to the different coefficients used in the theory.

References

[1] Ponomarenko, S.A., Agrawal, G.P.:Do Solitonlike Self-Similar Waves Exist in Nonlinear Optical Media? Phys. Rev. Lett. 97, 013901 (2006)

[2] Li, L., Zhao, X.S., Xu, Z.Y.: Dark solitons on an intense parabolic background in nonlinear waveguides. Phys. Rev. A 78, 063833 (2008)

[3] Luo, H.G., Zhao, D, He, X.G.: Exactly controllable transmission of nonautonomous optical solitons. Phys. Rev. A 79, 063802 (2009)

[4] Viscondi, T. F., Furuya, K.: Dynamics of a Bose-Einstein condensate in a symmetric triple-well trap. J. Phys. A: Math. Theor. 44, 175301 (2011)

[5] Kruglov, V.I., Peacock, A.C., Harvey J.D.: Exact Self-Similar Solutions of the Generalized Nonlinear Schrödinger Equation with Distributed Coefficients. Phys. Rev. Lett. 90, 113902 (2003)

[6] Serkin, V.N., Hasegawa, A., Belyaeva1, T.L.: Nonautonomous solitons in external potentials. Phys. Rev. Lett. 98, 074102 (2007)

[7] Ding, C.C., Gao, Y.T., Deng, G.F., Wang, D.: Lax pair, conservation laws, Darboux transformation, breathers and rogue waves for the coupled nonautonomous nonlinear Schrödinger system in an inhomogeneous plasma. Chaos Solitons Fract. 133, 109580 (2020)

[8] Wang, M., Tian, B.: In an inhomogeneous multicomponent optical fiber: Lax pair, generalized Darboux transformation and vector breathers for a three-coupled variable-coefficient nonlinear Schrödinger system. Eur. Phys. J. Plus. 136, 1002 (2021)

[9] Yang, D.Y., Tian, B., Wang, M., Zhao, X., Shan, W.R., Jiang, Y.: Lax pair, Darboux transformation, breathers and rogue waves of an N-coupled nonautonomous nonlinear Schrödinger system for an optical fiber or a plasma. Nonlinear Dyn. 107, 2657-2666 (2022)

[10] Yang, R.C., Gao, J., Jia, H.P., Tian, J.P., Christian, J.M.: Ultrashort nonautonomous similariton solutions and the cascade tunneling of interacting similaritons. Opt. Commun. 459, 125025 (2020)

[11] Wu, X.F., Hua, G.S., Ma, Z.Y.: Novel rogue waves in an inhomogenous nonlinear medium with external potentials. Commun. Nonlinear Sci. Numer. Simul. 18, 3325–3336 (2013)

[12] Perego, A.M.: Exact superregular breather solutions to the generalized nonlinear Schrödinger equation with nonhomogeneous coefficients and dissipative effects. Opt. Lett. 45(14), 3913 (2020)

[13] Triki, H., Choudhuri, A., Zhou, Q., Biswas, A., Alshomrani, A.S.: Nonautonomous matter wave bright solitons in a quasi-1D Bose-Einstein condensate system with contact repulsion and dipole-dipole attraction. Appl. Math. Comput. 371, 124951 (2020)

[14] Djoptoussia, C., Tiofack, C.G.L., Alim, Mohamadou, A., Kofané, T.C.: Ultrashort self-similar periodic waves and similaritons in an inhomogeneous optical medium with an external source and modulated coefficients. Nonlinear Dyn. 107, 3833-3846 (2022)

[15] Liu, C.P., Yu, F.j., Li, L.: Non-autonomous wave solutions for the Gross-Pitaevskii (GP) equation with a parabola external potential in Bose-Einstein condensates. Phys. Lett. A 383, 125981 (2019)

[16] Manikandan, K., Muruganandam, P., Senthilvelan, M., Lakshmanan, M.: Manipulating localized matter waves in multicomponent Bose-Einstein condensates. Phys. Rev. E 93, 032212 (2016)

[17] Mareeswaran, R.B., Kanna, T.: Superposed nonlinear waves in coherently coupled Bose–Einstein condensates. Phys. Lett. A 380: 3244–3252 (2016)

[18] Jia, H.P., Li, B., Yang, R.C., Tian, J.P.: Diverse composite waves in coherently coupled inhomogeneous fiber systems with external potentials. Nonlinear Dyn. 99(4), 2987-2999 (2020)

[19] Xue, R.R., Yang, R.C., Jia, H.P., Wang, Y.: Novel bright and kink similariton solutions of cubic-quintic nonlinear Schrödinger equation with distributed coefficients. Phys. Scr. 96, 125230 (2021)

[20] He, X.G., Zhao, D., Li, L., Luo, H.G.: Engineering integrable nonautonomous nonlinear Schrödinger equations. Phys. Rev. E 79, 056610 (2009)

[21] Nandy, S., Barthakur, A.: Dark-bright soliton interactions in coupled nonautonomous nonlinear Schrödinger equation with complex potentials. Chaos Soliton. Fract. 143, 110560 (2021)

[22] Agrawal, G.P.: Nonlinear Fiber Optics, 4th ed. Academic Press, New York (2007)

[23] Chabchoub, A., Hoffmann, N.P., Akhmediev, N.: Rogue wave observation in a water wave tank. Phys. Rev. Lett. 106(20), 204502 (2011)

[24] Chabchoub, A., Hoffmann, N., Onorato, M.: Akhmediev N. Super rogue waves: observation of a higher-order breather in water waves. Phys. Rev. X 2(1), 011015 (2012)

[25] Akhmediev, N., Ankiewicz, A., Soto-Crespo, J.M.: Rogue waves and rational solutions of the nonlinear Schrödinger equation. Phys. Rev. E 80, 026601 (2009)

[26] Ankiewicz, A., Kedziora, D.J., Akhmediev, N.: Rogue wave triplets. Phys. Lett. A 375, 2782–2785 (2011).

[27] Kengne, E., Lakhssassi, A., Liu, W.M.: Non-autonomous solitons in inhomogeneous nonlinear media with distributed dispersion. Nonlinear Dyn. 97, 449–469 (2019)

[28] Loomba, S., Kaur, H.: Optical rogue waves for the inhomogeneous generalized nonlinear Schrödinger equation. Phys. Rev. E 88, 062903 (2013)

[29] Kundu, A.: Integrable nonautonomous nonlinear Schrödinger equations are equivalent to the standard autonomous equation. Phys. Rev. E 79, 015601 (2009)

[30] Zhao, D., He, X.G., Luo, H.G.: From canonical to nonautonomous solitons, Eur. Phys. J. D 53, 213–216 (2009)

[31] Triki, H., Zhou, Q., Biswas, A., Xu, S.L., Alzahrani, A.K., Belic, M.R.: Self-frequency shift effect for chirped self-similar solitons in a tapered graded-indexed waveguide. Opt. Commun. 468, 125800 (2020)

[32] Dai, C.Q., Wang, Y.Y., Tian, Q., Zhang, J.F.: The management and containment of self-similar rogue waves in the inhomogeneous nonlinear Schrödinger equation. Ann. Phys. 327, 512–521 (2012)

[33] Kumar, C.N., Gupta, R., Goyal, A., Loomba, S., Raju, T.S., Panigrahi, P.K.: Controlled giant rogue waves in nonlinear fiber optics. Phys. Rev. A 86, 025802 (2012)

[34] Ponomarenko, S.A., Agrawal, G.P.: Optical similaritons in nonlinear waveguides. Opt. Lett. 32, 1659 (2007)

[35] Kengne, E., Liu, W.M.: Management of matter-wave solitons in Bose-Einstein condensates with time-dependent atomic scattering length in a time-dependent parabolic complex potential. Phys. Rev. E 98, 012204 (2018)

[36] Zhang, J.F., Hu, W.C.: Controlling the propagation of optical rogue waves in nonlinear graded-index waveguide amplifiers. Chin. Opt. Lett. 11(3), 031901 (2013)

[37] Kruglov, V.I., Triki, H.: Quartic and dipole solitons in a highly dispersive optical waveguide with self-steepening nonlinearity and varying parameters. Phys. Rev. A 102, 043509 (2020)

[38] Triki, H., Kruglov, V.I.: Chirped self-similar solitary waves in optical fibers governed with self-frequency shift and varying parameters. Chaos Soliton. Fract. 143, 110551 (2021)

[39] Jia, H.P., Yang, R.C., Tian, J.P., Zhang, W.M.: Controllable excitation of higher-order rogue waves in nonautonomous systems with both varying linear and harmonic external potentials. Opt. Commun. 415, 93–100 (2018)

[40] Mahato, D.K., Govindarajan, A., Lakshmanan, M., Sarma, A.K.: Dispersion managed generation of Peregrine solitons and Kuznetsov-Ma breather in an optical fiber. Phys. Lett. A 392, 127134 (2021)

[41] Tiofack, C.G.L., Coulibaly, S., Taki, M., Bièvre, S.D., Dujardin, G.: Periodic modulations controlling Kuznetsov–Ma soliton formation in nonlinear Schrödinger equations. Phys. Lett. A 381, 1999–2003 (2017)

[42] Zhao, D., Luo, H.G., Chai, H.Y.: Integrability of the Gross–Pitaevskii equation with Feshbach resonance management. Phys. Lett. A 372, 5644 (2008)

[43] Manikandan, K., Muruganandam, P., Senthilvelan, M., Lakshmanan, M.: Manipulating matter rogue waves and breathers in Bose-Einstein condensates. Phys. Rev. E 90, 062905 (2014)

[44] He, J., Li, Y.: Designable Integrability of the Variable Coefficient Nonlinear Schrödinger Equations. Stud. Appl. Math. 126, 1-15 (2011)

[45] Manikandan, K., Priya, N.V., Senthilvelan, M., Sankaranarayanan, R.: Higher-order matter rogue waves and their deformations in two-component Bose–Einstein condensates. Wave. Random Complex 32, 867-886. (2022)

[46] Hao, R.R., Li, L., Li, Z.H., Zhou, G.S.: Exact multisoliton solutions of the higher-order nonlinear

Schrödinger equation with variable coefficients. Phys. Rev. E 70, 066603 (2004)

[47] Yang, R.C., Li, L., Hao, R.Y., Li, Z.H., Zhou, G.S.: Combined solitary wave solutions for the inhomogeneous higher-order nonlinear Schrödinger equation. Phys. Rev. E 71: 036616 (2005)

[48] Chabchoub, A., Hoffmann, N., Onorato, M., Slunyaev, A., Sergeeva, A., Pelinovsky, E., Akhmediev, N.: Observation of a hierarchy of up to fifth-order rogue waves in a water tank. Phys. Rev. E 86, 056601 (2012)

Statements and Declarations

Funding This work was supported by the National Natural Science Foundation of China (Grant numbers. 61775126, 62071282).

Competing Interests The authors have no relevant financial or non-financial interests to disclose.

CRediT authorship contribution statement

Kui Huo: Methodology, Software, Data analysis, Writing-original draft. ***Rongcao Yang***: Conceptualization, Theoretical analysis, Supervision. ***Heping Jia***: Conceptualization, Validation, Writing-review & editing. ***Yingji He***: Writing-review & editing. ***J.M. Christian***: Writing-review & editing.

Data availability Our manuscript has no associated data.